Available online at www.sciencedirect.com
SCIENCE DIRECT
Bioorganic & Medicinal Chemistry Letters 16 (2006) 363–366
Bioorganic & Medicinal Chemistry Letters

Biomimetic synthesis and ultrastructural characterization of a zerovalent gold–hydroxyapatite composite

Yogita Gupta,[a] G. N. Mathur[b,*] and Sandeep Verma[a,*]

[a]*Department of Chemistry, Indian Institute of Technology Kanpur, Kanpur-208016, UP, India*
[b]*Department of Chemical Engineering, Indian Institute of Technology Kanpur, Kanpur-208016, UP, India*

Received 11 August 2005; revised 21 September 2005; accepted 28 September 2005
Available online 2 November 2005

Abstract—This manuscript describes one-pot, in situ synthesis of organoapatite-gold nanoparticle composite and its characterization by XRD, energy dispersive X-ray analysis, atomic force, and scanning electron microscopy. This methodology offers a different approach into the synthesis of zerovalent metal-mineral-phase nanocomposites having potential application as osteointegrative ceramics.

Hydroxyapatite (HA) $Ca_{10}(PO_4)_6(OH)_2$ is a biologically important mineral phosphate that occurs naturally in mammalian hard tissues including bones, dentine, shells, and skeletal units as their mineral component.[1] Polyanionic proteins ensure controlled nucleation and modified growth of HA crystals in vivo,[2] resulting in two-dimensional growth of the nanocrystalline phase via ionic interactions between negatively charged carboxylate functionality and positively charged inorganic precursor mineral, octacalcium phosphate (OCP). The role of acidic organic templates and organogels for the synthesis of bone-like materials has been thoroughly investigated and interestingly, polyanionic nature of DNA has also been explored for the inhibition of the apatitic crystal growth.[3,4]

An emerging area within biomineralization concerns deposition of mineral phase leading to the generation of novel materials with desired composition and defined aggregational patterns.[5] Impregnation of biomimetic composites with zerovalent metals and metal oxides may impart interesting properties such as toughness and electrical conduction to these composites.

We have been interested in creating nucleobase polymers to study their ability to catalyze important chemical and biochemical transformations.[6] In order to broaden the catalytic profile of nucleobase polymers, we decided to equip them with amino acid side chains such as carboxylic group, primary amines, and alcohols. In this context, nucleobase polymer AP-1 was designed to bear pendant carboxyl groups (Fig. 1) and its activity was evaluated for controlled hydrolysis of octacalcium phosphate to mimic biological calcification by acidic proteins. The molecular skeleton of AP-1 combines carboxylic acid functionalities present in acidic proteins as well as polyanionic nature and nucleobase composition of DNA, which have been shown to catalyze biomineralization process. This is the justification for using AP-1 as a modulating polymer for OCP hydrolysis and composite synthesis.[3,4]

Herein, we report AP-1 controlled in situ synthesis of polymer-hydroxyapatite-gold nanoparticle composite and study of their ultrastructural details via various microscopic techniques.

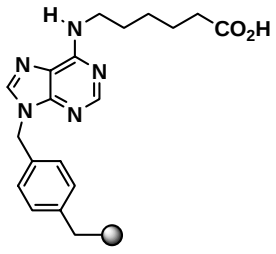

Figure 1. Structural representation of AP-1.

Keywords: Purine; Adenine; Polymer; Apatite.
* Corresponding authors. Tel.: +91 512 259 7643; fax: +91 512 259 7436; e-mail: sverma@iitk.ac.in

0960-894X/$ - see front matter © 2005 Elsevier Ltd. All rights reserved.
doi:10.1016/j.bmcl.2005.09.074

The experimental protocol used in this study enabled a facile access to an apatitic composite with possible biomedical applications. We have employed a negatively charged nucleobase polymer AP-1 as a novel modulator to access controlled growth of the apatitic phase. AP-1 was synthesized via conventional AIBN-mediated polymerization condition and its molecular weight was determined by GPC measurements.[7]

AP-1 was used to modulate the hydrolysis of octacalcium phosphate to hydroxyapatite and also for the growth of apatitic phase in the presence of gold nanoparticles.[7] The envisaged role of negatively charged polymer, akin to acidic proteins, is to bind to OCP phase and retard its hydrolysis. Subsequent to OCP hydrolysis in the presence of AP-1, energy-dispersive X-ray (EDX) spectrum of HA–gold composite was recorded to confirm the presence and relative ratio of various constituents in the composite (Fig. 2).[8] Although it was difficult to identify metallic gold phase as it overlapped with the more intense phosphorus peak, a calcium-to-phosphate ratio (Ca/P) of 1.33 and 1.65 was calculated for OCP and HA crystals, respectively, as expected for the compositions of OCP and HA.[9] Typical apatitic features were observed in XRD patterns and FTIR spectra (data not shown). Significantly, there was no change in the XRD pattern of HA when the reaction was performed in the presence of gold nanoparticles, indicating a lack of interference with HA crystal faces.

AFM micrographs provided crucial insight into the morphology of the mineral phase and adsorption of gold nanoparticles to yield nanocomposites. Two different ultrastructural HA morphologies, fiber and spherule-like, were evident from AFM studies (Figs. 3 and 4).[10] Highly aggregated long HA nanofibers with an

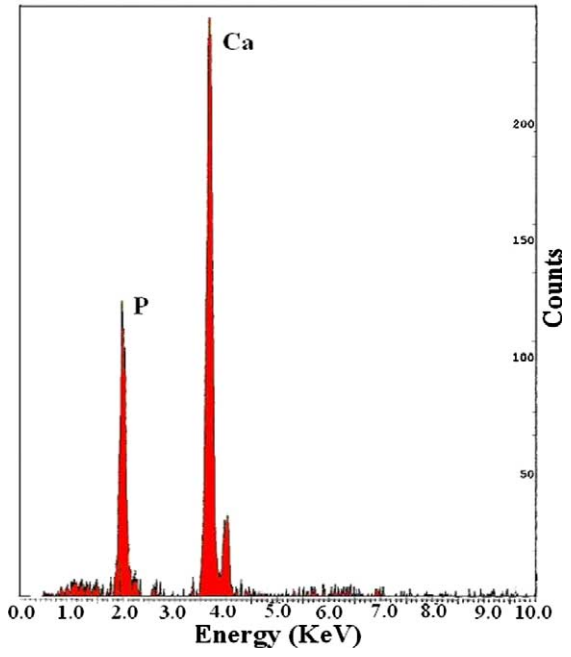

Figure 2. EDX spectrum of HA–gold composite.

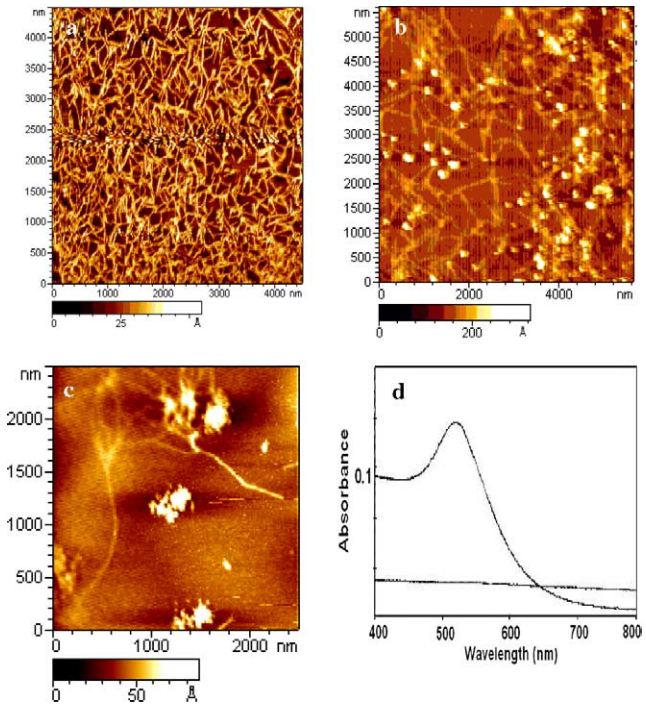

Figure 3. AFM micrographs of HA: (a) and (b), in the absence and presence of gold nanoparticles, respectively (AP-1 = 0.001 mg/mL); (c) magnified HA–gold composite (AP-1 = 0.1 mg/mL); (d) UV–Visible spectra of gold nanoparticles in the absence (i) or presence of HA/OCP (ii).

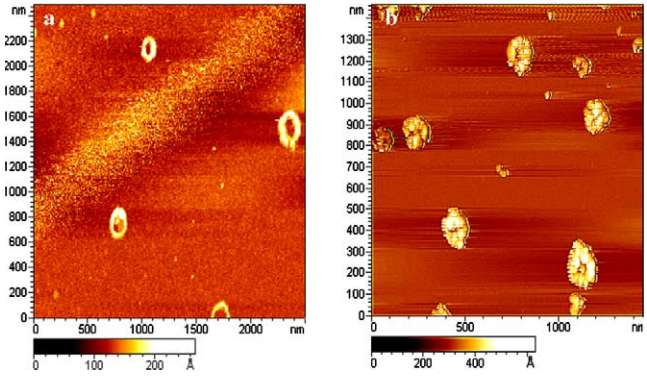

Figure 4. AFM images (a) and (b) of HA spherules in the absence and presence of gold, respectively.

average width of ~50 nm were observed for AP-1 concentration of 0.001 mg/mL (Fig. 3a). This morphology varied with different AP-1 concentrations indicating highly controlled OCP hydrolysis (data not shown). When this experiment was performed with gold nanoparticles, they tend to get adsorbed on HA fibers and appeared as bright spots (~140 nm width) (Fig. 3b). These particles appeared to mostly aggregate along the length of the apatite fiber (Fig. 3c). In both cases, a distinct loss of surface plasmon band of gold nanoparticles, subsequent to their adsorption on HA surface, was taken as an indication of gold adsorption and its interaction with the mineral interface, thus causing a shift in its optical behavior compared to that of its free colloidal solution (Fig. 3d). These observations are similar to a recent

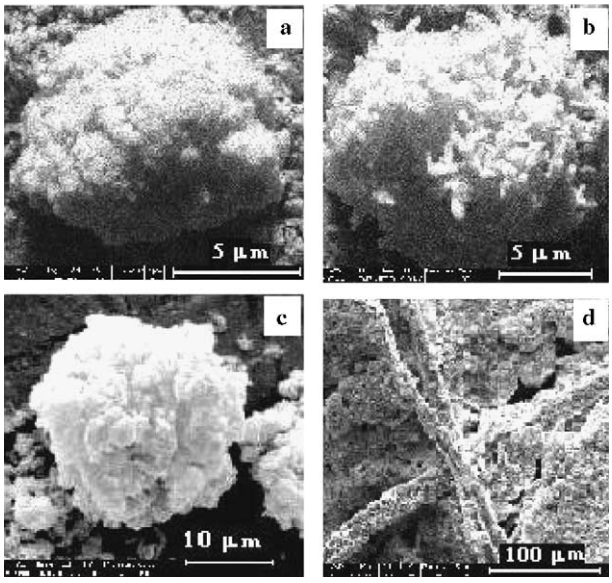

Figure 5. SEM images of (a) HA alone; (b) and (c) polymer–HA–gold composite synthesized using 0.001 and 1.0 mg/mL AP-1, respectively; (d) fibrous morphology of polymer–HA–gold composite.

elegant demonstration of HA crystal synthesis using amino acid-capped gold nanoparticles by Sastry and co-workers.[11]

A spherule-like morphology for HA alone was also observed (Fig. 4a), while its synthesis in the presence of gold nanoparticles revealed decoration of spherules with nanoparticles, displaying an average width and height (*Z*-scale) of ~130 and 190 nm, respectively (Fig. 4b). A facile, controlled synthesis of HA composites, containing gold particles, offers a versatile entry into electroconductive osteointegrative materials.

AFM micrographs once again revealed that the adsorption of gold colloids does not affect overall morphology of HA crystal by simply getting deposited on HA surface, as evidenced by the 'lighted' spherules. The ease of in situ deposition of gold nanoparticles on hydroxyapatite spherules is notable and presents an attractive method for the construction of bioactive metal-hydroxyapatite (mineral) composites.

SEM micrographs further confirmed spherule-like and fibrous morphologies of HA, under AP-1 controlled synthesis, in the presence or absence of gold nanoparticles (Figs. 5a–d).[12]

Finally, we probed thermal stability of the composite by thermogravimetric measurements. Initial degradation at 95 °C indicated water loss, followed by significant degradation at 340 °C (data not shown).[13] This suggests that controlled growth, deposition, and calcination of hydroxyapatite-gold composites might lead to robust and functional materials.

Control experiments were conducted with adenine polymer lacking the acidic side chain and with the monomer 9-(4-vinylbenzyl)-purin-6-yl-aminocaproic acid. Uncharged polymer failed to modulate hydrolysis, while the monomer did not retard the reaction to the extent of AP-1 (data not shown). This confirms the role of multiple negative charges in a polymeric scaffold for the inhibition of OCP hydrolysis.

Gold interacts favorably with biomolecules reflecting on its wide-ranging biological applications in diagnostics and nanobiotechnology.[14] However, innovations in novel colloidal gold-based materials are also required for other applications.[15] Furthering this theme, we have presented a facile one-pot, in situ synthetic approach and characterization for novel polymer–HA–gold nanoparticle composite. This benign method offers simplicity and a viable alternative compared to other reported methods. From another standpoint, this method points toward plausible alternative processes for biomineralization prior to the evolution of specialized proteins for this purpose.

It is believed that apatitic composites with zerovalent metals will be useful in the design and construction of devices, biosensors, prosthetics, and implants with superior mechanical properties, and as catalysts. We are currently undertaking detailed physico-mechanical and functional characterization of such composites.

Acknowledgments

We thank Prof. A. Sharma, Department of Chemical Engineering, Prof. V. Chandrasekhar, Department of Chemistry, and ACMS, IIT-Kanpur, for instrumentation. Financial support from Department of Science and Technology, India, to one of us (S.V.) is gratefully acknowledged.

References and notes

1. (a) Kaito, T.; Myoui, A.; Takaoka, K.; Saito, N.; Nishikawa, M.; Tamai, N.; Ohgushi, H.; Yoshikawa, H. *Biomaterials* **2005**, *26*, 3; (b) Chen, Q. Z.; Wong, C. T.; Lu, W. W.; Cheung, K. M. C.; Leong, J. C. Y.; Luk, K. D. K. *Biomaterials* **2004**, *25*, 4243; (c) Robinson, C.; Connell, S.; Kirkham, J.; Shorea, R.; Smith, A. *J. Mater. Chem.* **2004**, *14*, 2242.
2. (a) Bouropoulos, N.; Moradian-Oldak, J. *J. Dent. Res.* **2004**, *83*, 278; (b) He, G.; Dahl, T.; Veis, A.; George, A. *Nat. Mater.* **2003**, *2*, 552; (c) Heiss, A.; DuChesne, A.; Denecke, B.; Grotzinger, J.; Yamamoto, K.; Renne, T.; Jahnen-Dechent, W. *J. Biol. Chem.* **2003**, *278*, 13333; (d) Kawasaki, K.; Kambara, M.; Matsumura, H.; Norde, W. *Colloids Surfaces B* **2003**, *32*, 321.
3. (a) Bigi, A.; Bracci, B.; Panzavolta, S.; Iliescu, M.; Plouet-Richard, M.; Werckmann, J.; Cam, D. *Cryst. Growth Des.* **2004**, *4*, 141; (b) Estroff, L. A.; Addadi, L.; Weiner, S.; Hamilton, A. D. *Org. Biomol. Chem.* **2004**, *1*, 137; (c) Bigi, A.; Boanini, E.; Bracci, B.; Falini, G.; Rubini, K. *J. Inorg. Biochem.* **2003**, *95*, 291; (d) Tsortos, A.; Nancollas, G. H. *J. Colloid Interface Sci.* **2002**, *250*, 159.
4. Okazaki, M.; Yoshida, Y.; Yamaguchi, S.; Kaneno, M.; Elliott, J. C. *Biomaterials* **2001**, *22*, 2459.
5. Kim, H-M. *Curr. Opin. Solid State Mater. Sci.* **2003**, *7*, 289.

6. (a) Madhavaiah, C.; Verma, S. *Chem. Commun.* **2003**, *6*, 800; (b) Srivatsan, S. G.; Parvez, M.; Verma, S. *Chem. Eur. J.* **2002**, *8*, 5184.
7. All glasswares were thoroughly cleaned with a detergent, aqua regia, and finally with repeated washings with double distilled water. They were finally rinsed with triple distilled water and oven-dried before use. *Poly-(9-(4-vinylbenzyl)-purin-6-yl)-amino caproic acid (AP-1)*. 9-(4-Vinylbenzyl)-purin-6-yl-amino caproic acid (1.0 g, 2.7 mmol) was dissolved in dry DMSO (10 mL) and AIBN (13 mg) added to it. Reaction mixture was degassed by purging oxygen-free nitrogen for 1 h, followed by three cycles of freeze thawing. Polymerization reaction was performed at 80 °C for 24 h under nitrogen atmosphere. AP-1 was precipitated by adding methanol (70 mL) and was filtered. Precipitated AP-1 was dissolved in a minimum amount of DMSO and reprecipitated with methanol. The process was repeated three times and finally, AP-1 was washed with methanol (5×20 mL), chloroform (5×20 mL), acetone (2×20 mL), and ether, and dried under vacuum (0.6 g, yield 60% by weight). The molecular weight of AP1 was obtained from gel permeation chromatography. Weight-average (M_w) and number-average molecular weights (M_n) were found to be 68,800 and 35,000 Da, respectively, with $M_w/M_n = 1.96$. *OCP synthesis and characterization*. OCP hydrolysis was carried out in the presence of AP-1 sodium salt at various polymer concentrations (0.001, 0.1 or 1.0 mg/mL) in nanopure water at pH 7.4, maintaining the temperature at 70 °C for 48 h. The white colored product so obtained was filtered, repeatedly washed with nanopure water, and dried at 37 °C. *Synthesis of gold nanoparticles.* Gold nanoparticles were prepared by standard borohydride reduction method to access smaller particle size. 4% chloroauric acid solution (375 μL) and 0.2 M K_2CO_3 (500 μL) were prepared in triple distilled water. Both of these solutions were added to 100 mL triple distilled water and the mixture was cooled to 4 °C, with continuous stirring. Five milliliter aliquots of $NaBH_4$ (2.5 mg of $NaBH_4$ in 5 mL water) were added to the reaction mixture and stirring was continued for 5 min. Formation of gold nanoparticles was indicated by the color change. This solution was stored and used in reactions. *OCP hydrolysis in the presence of gold nanoparticles*. This reaction was carried out in the presence of AP-1 sodium salt at three different concentrations (0.001, 0.1 or 1 mg/mL), in the presence of gold nanoparticle solution (1.8 mg/L) at pH 7.4, by maintaining the temperature at 70 °C for 48 h. A pink colored product appeared in the case of added gold particle solution, which was filtered and repeatedly washed with double distilled water and dried at 37 °C. Morphology of the product so obtained was studied by powder X-ray diffraction and other microscopic techniques.
8. *Powder X-ray diffraction analysis*. The samples were scanned from 5 to 60° in 2θ ranges at a scanning speed of 3.0°/min with ISO-Debyeflex 2002 powder diffractometer, equipped with graphite monochromator in the diffracted beam. Cu–K_α radiation was generated at 30 kV and 20 mA. Typical apatitic features were observed. A small double peak immediately below 10° belonging to (1 1 0) and (0 1 0) OCP reflections was present in the precursor mineral phase (data not shown).
9. (a) Kim, H-M.; Himeno, T.; Kawashita, M.; Kokubo, T.; Nakamura, T. *J. R. Soc. Lond. Interface* **2004**, *1*, 17; (b) Wang, H.; Lee, J. K.; Moursi, A.; Lannutti, J. J. *J. Biomed. Mat. Res.* **2003**, *67A*, 599.
10. *Atomic force microscopy*. The samples were imaged with an atomic force microscope (Molecular Imaging, USA), operating in the Acoustic AC mode (AAC) with the aid of a cantilever NSC12 (E) (MikroMasch). The force constant was 0.3 N/m, while the resonant frequency used was 24 kHz. The images were taken in air at room temperature, with a scan speed of 1.5–2.2 lines/s. Data acquisition was performed by PicoScan 5® software and the analysis was done with the aid of visual SPM. Hydrolysis products in double distilled water were ultrasonicated and a drop of suspension was transferred onto freshly cleaved mica and dried under nitrogen flow, prior to imaging.
11. Rautaray, D.; Mandal, S.; Sastry, M. *Langmuir* **2005**, *21*, 5185.
12. *Scanning electron microscopy and EDAX analysis*. Samples were gold sputter-coated prior to imaging and the scanning was carried out with FEI QUANTA 200 scanning microscope to observe size and morphology of the samples. However, energy dispersive X-ray was taken using copper stubs as the composite contained colloidal gold.
13. *Thermogravimetric analysis*. The sample weights were in the range of 1–8 mg. TGA was carried out using a Perkin-Elmer TGA-6 instrument. Heating was performed in a platinum crucible under nitrogen flow (60 cm^3/min) at a rate of 5 °C/min up to 900 °C.
14. (a) Schmid, G.; Simon, U. *Chem. Commun.* **2005**, *6*, 697; (b) Thaxton, C. S.; Mirkin, C. A. *Nanobiotechnology* **2004**, 288; (c) Niemeyer, C. M. *Biochem. Soc. Trans.* **2004**, *32*, 51; (d) Penn, S. G.; He, L.; Natan, M. J. *Curr. Opin. Chem. Biol.* **2003**, *7*, 609; (e) Sastry, M.; Rao, M.; Ganesh, K. N. *Acc. Chem. Res.* **2002**, *35*, 847.
15. (a) Chen, M. S.; Goodman, D. S. *Science* **2004**, *306*, 252; (b) Haruta, M. *Gold Bull.* **2004**, *37*, 27; (c) Kulkarni, G. U.; Vinod, C. P.; Rao, C. N. R. *Surface Chem. Catal.* **2002**, 191; (d) Valden, M.; Lai, X.; Goodman, D. W. *Science* **1998**, *281*, 1647.